ORIGINAL ARTICLE

Journal of Neurochemistry | JNC The Official Journal of the International Society for Neurochemistry | WILEY

Dopamine promotes the neurodegenerative potential of β-synuclein

Anupam Raina[1] | Kristian Leite[1] | Sofia Guerin[1] | Sameehan U. Mahajani[1] |
Kalyan S. Chakrabarti[2] | Diana Voll[1] | Stefan Becker[2] | Christian Griesinger[2] |
Mathias Bähr[1] | Sebastian Kügler[1,3]

[1]Department of Neurology, University Medicine Göttingen, Göttingen, Germany

[2]Max-Planck-Institute for Biophysical Chemistry, Göttingen, Germany

[3]Center Nanoscale Microscopy and Physiology of the Brain (CNMPB), Göttingen, Germany

Correspondence
Sebastian Kügler, Department of Neurology, University Medicine Göttingen, Waldweg 33, 37073 Göttingen, Germany.
Email: sebastian.kuegler@med.uni-goettingen.de

Present address
Anupam Raina, Department of Molecular Biology, UT Southwestern Medical Center, Dallas, TX, USA
Sameehan U. Mahajani, Department of Pathology, Stanford University, Stanford, CA, USA
Kalyan S. Chakrabarti, Division of Sciences, Krea University, Sri City, India

Abstract

A contribution of α-Synuclein (α-Syn) to etiology of Parkinson´s disease (PD) and Dementia with Lewy bodies (DLB) is currently undisputed, while the impact of the closely related β-Synuclein (β-Syn) on these disorders remains enigmatic. β-Syn has long been considered to be an attenuator of the neurotoxic effects of α-Syn, but in a rodent model of PD β-Syn induced robust neurodegeneration in dopaminergic neurons of the substantia nigra. Given that dopaminergic nigral neurons are selectively vulnerable to neurodegeneration in PD, we now investigated if dopamine can promote the neurodegenerative potential of β-Syn. We show that in cultured rodent and human neurons a dopaminergic neurotransmitter phenotype substantially enhanced β-Syn-induced neurodegeneration, irrespective if dopamine is synthesized within neurons or up-taken from extracellular space. Nuclear magnetic resonance interaction and thioflavin-T incorporation studies demonstrated that dopamine and its oxidized metabolites 3,4-dihydroxyphenylacetaldehyde (DOPAL) and dopaminochrome (DCH) directly interact with β-Syn, thereby enabling structural and functional modifications. Interaction of DCH with β-Syn inhibits its aggregation, which might result in increased levels of neurotoxic oligomeric β-Syn. Since protection of outer mitochondrial membrane integrity prevented the additive neurodegenerative effect of dopamine and β-Syn, such oligomers might act at a mitochondrial level similar to what is suggested for α-Syn. In conclusion, our results suggest that β-Syn can play a significant pathophysiological role in etiology of PD through its interaction with dopamine metabolites and thus should be re-considered as a disease-relevant factor, at least for those symptoms of PD that depend on degeneration of nigral dopaminergic neurons.

1 | INTRODUCTION

The synuclein family of proteins consists of three members, α-Synuclein (α-Syn), β-Synuclein (β-Syn), and γ-Synuclein (γ-Syn). α-Syn is closely linked to the etiology of PD, as mutations, enhanced gene dosage, and single nucleotide polymorphisms causing subtle increases in protein levels all result in aggravated PD symptoms. In addition, α-Syn is a major component of proteinaceous aggregate structures, Lewy bodies, and Lewy neurites, that are found in all genetic and idiopathic cases of PD (Galvin, Lee, & Trojanowski, 2001; Poewe et al., 2017). γ-Syn accumulations have been detected in human brains, sometimes co-localizing with α-Syn (Surgucheva, Newell, Burns, & Surguchov, 2014). β-Syn aggregates have not yet been detected in human brain (Spillantini & Goedert, 2018), and the role of β-Syn in human brain disorders is currently enigmatic.

The degeneration of dopaminergic A9 neurons of the substantia nigra pars compacta (SNpC) constitutes a major hallmark of Parkinson´s disease (PD). Loss of these neurons causes prominent motor symptoms like tremor, rigidity, postural instability, and inability to initiate movements. No formal proof exists yet to declare α-Syn directly responsible for degeneration of nigral dopaminergic neurons in PD patients (Espay et al., 2019). However, the intimate link of α-Syn to etiology of PD and the specific degeneration of A9 neurons suggest a likely connection between α-Syn and the presence of dopamine (DA), which henceforth we describe as the dopaminergic neurotransmitter phenotype of these cells. This dopaminergic neurotransmitter phenotype is a risk factor for neurodegeneration by itself, because of the oxidative stress that results from dopamine metabolism and auto-oxidation (Jinsmaa, Sharabi, Sullivan, Isonaka, & Goldstein, 2018). Several studies have demonstrated that DA, or rather its oxidized metabolites, can interact with α-Syn, thereby enhancing the neurotoxic potential of the protein by inhibiting fibril formation and promoting formation of disease-relevant oligomeric species (Asanuma, Miyazaki, & Ogawa, 2003; Burke, Kumar, & Pandey, 2008; Cappai, Leck, & Tew, 2005; Mor, Daniels, & Ischiropoulos, 2019; Mor, Tsika, & Mazzulli, 2017; Pham et al., 2009; Planchard, Exley, Morgan, & Rangachari, 2014). Furthermore, both enzymatic and auto-oxidation of DA results in production of cytotoxic molecules like hydrogen peroxide and reactive aldehydes, with very high potential to oxidatively damage proteins, lipids, and DNA.

β-Syn, closely related to α-Syn but partially lacking the central aggregation-promoting part known as the NAC-domain (amino acids 61–95 in α-Syn, amino acids 73–83 lacking in β-Syn) (Giasson, Murray, Trojanowski, & Lee, 2001), is expressed in mammalian brain to similar extent as α-Syn (Kasten & Klein, 2013), in a 1:1 ratio with α-Syn in rodent brain synaptic boutons (Wilhelm et al., 2014). β-Syn has long been thought to serve as an anti-aggregating and potentially neuroprotective counterpart to α-Syn (Fan et al., 2006; Giasson et al., 2001; Hashimoto et al., 2004; Park & Lansbury, 2003; Uversky et al., 2002). Contrasting this view, β-Syn has been shown to be capable of aggregating in cell-free assays because of macromolecular crowding and interaction with metal ions and pesticides (Yamin et al., 2005), and because of acidic pH (Moriarty et al., 2017) and interaction with lipid vesicles at elevated temperatures (Brown et al., 2018). In vivo, it was recently shown that β-Syn forms proteinase K resistant fibrils in dopaminergic neurons of the rat substantia nigra and causes degeneration of these neurons to a similar extent as α-Syn (Taschenberger et al., 2013). Studies in cultured non-dopaminergic neurons have demonstrated that the general mechanism of neurodegeneration induced by β-Syn converges on permeation of the outer mitochondrial membrane (OMM) followed by cytochrome C-mediated caspase activation (Tolö et al., 2018). However, it remains unknown up to now, if DA and its metabolism can influence the neuropathological profile of β-Syn. If so, this would place β-Syn at a central position when trying to understand the reasons for preferential degeneration of nigral A9 neurons in PD.

To study the neurodegenerative potential of β-Syn in presence or absence of DA, we generated cell cultures allowing to exploit neurons that are identical in *verum* and control conditions except for the presence or absence of DA. Such cells are not naturally available. Genuine dopaminergic neuron cultures isolated from rodent midbrains contain only a small percentage of dopaminergic neurons in a background of about 90% GABAergic neurons, and the dopaminergic cell population can only be identified after fixation and immunocytochemistry. More importantly, no controls are available for these neurons, which are differing from the dopaminergic phenotype solely by absence of dopamine synthesis. As such, we established rodent and human neuron cultures that express various parts of the dopamine synthesis and uptake machinery. AAV viral vectors were used for this purpose in rodent primary neurons, and also allowed for expression of the synucleins and fluorescent markers in both, rodent and human neurons. These attempts created a complex, but still highly versatile cell culture system allowing to evaluate the impact of DA on neurotoxic aspects of β-Syn.

We report that both intracellular DA synthesis and uptake of extracellular DA promote β-Syn-induced neurodegeneration, and that oxidized metabolites of DA physically interact with β-Syn, allowing for modification of the aggregation propensities of β-Syn. These results demonstrate that the neuropathological profile of β-Syn is substantially enhanced by DA, suggesting that an interplay of β-Syn and DA may promote loss of dopaminergic neurons in PD and DLB.

2 | MATERIALS AND METHODS

2.1 | Primary neuron culture

Primary neuron/glia co-cultures were prepared from rat embryonal E18 cortex and cultured essentially as described (Kügler et al. 2003). Briefly, cortices were mechanically dissociated, and single cell

suspensions were prepared by digestion with trypsin and DNAse. After a short incubation in fetal calf serum to inhibit trypsin activity, cells were triturated through a fire-polished glass capillary, debris removed by gravitational sedimentation, cells were counted and seeded at 250.000 cells/well in 24-well plates. The cell culture medium of 750 μl/well was not exchanged or further supplemented during the course of the experiments except for addition of L-DOPA or DA. For preparation of primary neurons from embryonic rat brains, all experimental animal procedures in Wistar rats (RRID:RGD_13508588; provided by the Central Animal Facility of University Medicine Göttingen) were conducted according to approved experimental animal licenses issued by the responsible animal welfare authority (Niedersächsisches Landesamt für Verbraucherschutz und Lebensmittelsicherheit, LAVES) and controlled by the local animal welfare committee and veterinarians of University Medical Center Göttingen. Pregnant females were about 3–5 months of age, weighted about 250–280 g, and were housed individually with ad libitum access to food and water. 55 such rats were used to prepare primary neurons from their embryos.

2.2 | Generation of hiPSCs

The CT-03 iPSC line was derived from a healthy 57-year old female. This line was generated from dermal skin fibroblasts, by Sendai virus-mediated transcription factor expression. Patterning into dopaminergic neurons or glutamatergic neurons was performed essentially as described (Kriks et al., 2011) (Vazin et al., 2014) with the modifications specified in (Mahajani, Raina, Fokken, Kügler, & Bähr, 2019), as shown in Figure 4a and b. Cells were seeded at 150.000 cells/well in 24-well plates. After completing the differentiation step the cell culture medium of 750 μl was not exchanged or further supplemented during the course of the experiments.

2.3 | AAV vectors

Recombinant AAV-6 vectors were produced as described (Tolö et al., 2018). Briefly, vector genome plasmids were co-transfected with the pDP6 helper plasmid into HEK293 cells (RRID:CVCL_6871), viral particles were harvested at 48 hr after transfection by three freeze-thaw cycles, pre-purified on an iodixanol step gradient, and purified and concentrated further by heparin affinity chromatography. After dialysis against PBS, single use aliquots were stored at −80°C in LoBind tubes (Eppendorf). Vector genome titers were determined by qPCR and purity >98% verified by SDS gel electrophoresis. All transgenes were expressed under control of the human synapsin 1 gene promoter (hSyn1), which provides strict neuron-specific expression (Kügler *et al.* 2003). Equal expression levels of all synucleins were verified for early time points of the study at div9, that is, before onset of neurodegeneration, by western blots of transduced neurons (Figure 1c). For the late time points of the study (i.e. after div 11, when

different extents of neurodegeneration became evident, this approach is likely to be inaccurate, because of different numbers of surviving neurons. Thus, we also verified equal expression levels by assessing the half-life of α-, β-, and γ-Syn in primary neurons, by exploiting a regulable vector system as described in Figure S1. Of note, these regulable vectors were used solely to address stability of the synucleins, and only constitutive synuclein expression was used to study the interactions with dopamine.
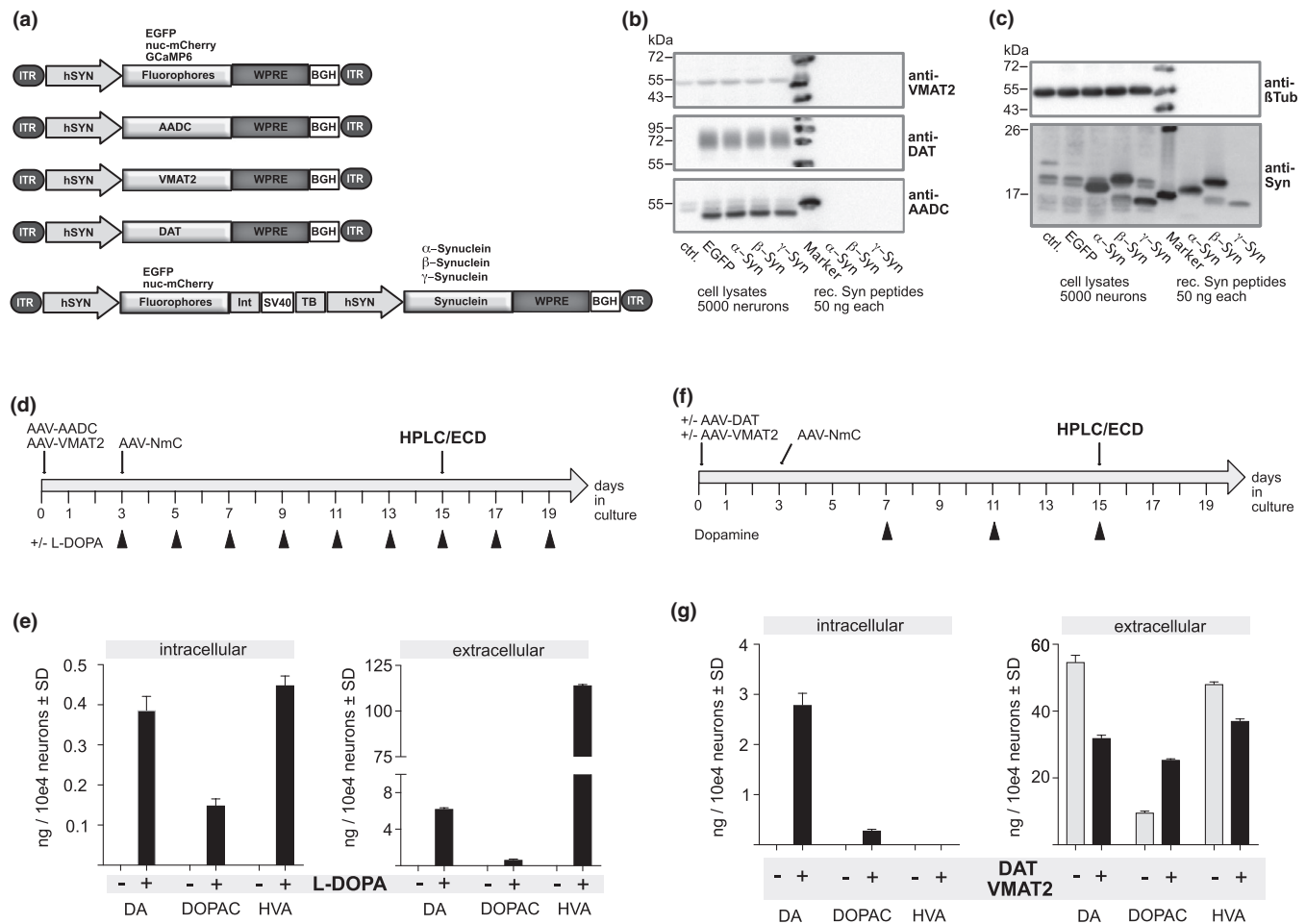
2.4 | Dopaminergic neuron models

Primary neurons were transduced with AAV vectors as follows: mono-cistronic vectors expressing AADC, VMAT2, DAT, Bcl-Xl, GCaMP6, or the nuclear mCherry fluorophore (Figure 1a) were added to primary neurons at times of preparation of the cells, by mixing 9×10^8 vg each with 250.000 cells per well to be seeded. After incubation with gentle shaking for 30 min at 37°C, cells were pelleted by centrifugation with 800 *g* to wash off residual virus, resuspended in cell culture medium and seeded. AAVs expressing the synucleins plus EGFP from a separate transcription unit were added into the cell culture medium on div 3 at a titer of 6×10^9 vg/well.

For generation of a cellular model of intracellular DA production, primary rat neuron cultures expressing AADC/VMAT2 were supplied with 10 μM L-DOPA every second day, starting from div3. Of note, it proved essential to allow for conversion of L-DOPA into DA, as in absence of AADC/VMAT2, L-DOPA itself caused significant neuron loss in these cultures (Figure S2). For generation of a cellular model of up-take of DA from extracellular space, primary rat neurons expressing DAT/VMAT2 were supplied with 12.5 μM DA every fourth day from div7 onwards.

Human iPSC-derived dopaminergic and glutamatergic neurons were transduced on DIV 20 (i.e. at the same time after starting the differentiation process for dopaminergic and glutamatergic neurons). Bi-cistronic vectors expressing α-Syn and EGFP, β-Syn and EGFP, γ-Syn and EGFP, or EGFP alone (Figure 1a) were added to the cells at 3×10^9 vg/ well.

2.5 | Imaging

Live cell imaging of spontaneous neuronal activity and for determination of surviving neuron numbers (as determined by presence of fluorescent markers) was performed on a Zeiss Observer Z1 microscope with heated stage and CO_2 incubation chamber, equipped with an AxioCam503 camera and ZEN 2.3 software. For data analysis, images were segmented in ImageJ using a custom-made macro with two steps of thresholding. In the first step, the image was segmented using the local thresholding method described by Phansalkar et al., with the following parameters—Phansalkar radius of 20 pixels, parameter 1 of 0.01 and parameter 2 of 100 (Phansalkar, More, Sabale, & Joshi, 2011). Following this, the dimmer

FIGURE 1 Generation of dopaminergic neurotransmitter phenotypes in primary neurons. (a) Schematic depiction of AAV vectors used in this study. Mono-cistronic constructs express fluorophores or factors essential for DA synthesis, uptake and sequestration, and bi-cistronic constructs express fluorophores and synucleins from independent transcription units. ITR = inverted terminal repeats of AAV-2; hSYN = human synapsin 1 gene promoter; WPRE = woodchuck hepatitis virus posttranscriptional control element; BGH = bovine growth hormone polyadenylation site; INT = synthetic intron; SV40 = Simian Virus 40 polyadenylation site. (b) Western blots of protein lysates obtained at div 9 from neurons transduced with AAVs expressing VMAT2, DAT and AADC plus AAVs expressing either only EGFP, α-Syn + EGFP, β-Syn + EGFP, γ-Syn + EGFP or no protein (ctrl.), stained with antibodies directed against either VMAT2, DAT or AADC. Blots demonstrate the AAV-mediated expression levels of VMAT2 (2-fold increase over endogenous level), DAT (not detectable in non-transduced neurons), and AADC (not detectable in non-transduced neurons). (c) Western blots of protein lysates obtained at div 9 from neurons transduced as in (b) to demonstrate the AAV vector-mediated overexpression of α-Syn (6-fold over endogenous level), β-Syn (5 - fold over endogenous level) and γ-Syn (level of overexpression not readily determinable, because of lack of an antibody that stains endogenous rat and overexpressed human γ-Syn with identical avidity). ctrl. = non-transduced neurons; EGFP = neurons expressing only EGFP; α-Syn = neurons expressing α-Syn + EGFP, β-Syn = neurons expressing β-Syn + EGFP, γ-Syn = neurons expressing γ-Syn + EGFP; rec. Syn peptides = recombinant α-, β-, and γ-Syn peptides, 50 ng/lane. Cell lysates loaded correspond to the protein equivalent of about 5,000 neurons. (d) Schematic depiction of the strategy used for intracellular DA synthesis by AADC/ VMAT2 expression. Triangles represent times of addition of L-DOPA. DA and metabolites DOPAC and HVA were quantified at div 15 by HPLC with electrochemical detection, as shown in (e). AAV-NmC (expressing nuclear-targeted mCherry) was used to allow for quantification of neuron numbers. (e) Intracellular and extracellular levels of DA, DOPAC, and HVA, obtained without (gray bars; values below detection limit) or with (black bars) addition of L-DOPA in neurons expressing AADC/ VMAT2. (f) Schematic depiction of the strategy used for up-take of DA from extracellular space by DAT/ VMAT2 expression. Triangles represent times of addition of DA. DA and metabolites DOPAC and HVA were quantified at div 15 by HPLC with electrochemical detection, as shown in (g). AAV-NmC (expressing nuclear-targeted mCherry) was used to allow for quantification of neuron numbers. (g) Intracellular and extracellular levels of DA, DOPAC and HVA, obtained without (gray bars; intracellular levels below detection limit) or with (black bars) expression of DAT and VMAT2. $N = 4–8$ independent neuron cultures per condition. Bars represent means $\pm$ SD

components of the image were thresholded again using the same method for the identification of nuclei with a low fluorescence. Then, particles larger than 120 pixels were identified and binarized, with clusters in the binary images separated into individual particles using the local maxima of fluorophore signals. Finally, the resulting number of particles was counted.

Calcium imaging exploiting the genetically encoded GCaMP6 sensor was performed essentially as described (Tolö et al., 2018).

2.6 | Western blotting

Protein lysates were obtained from transduced primary neurons by lysis in 50 mM Tris, pH 8.0, 0.5% SDS, 1 mM DTT and protease inhibitors Complete Mini, Roche). Samples were run in 12% SDS-PAGE and were blotted to PVDF membranes (fixed with 4% formaldehyde/ 0.4% glutaraldehyde in case of detection of the synucleins), blocked in non-fat dry milk or BSA in TBS-T, and incubated in TBS-T with the following primary antibodies at 4°C for 12 hr in roller tubes: anti pan-Synuclein (Abcam ab6176; RRID:AB_305344), anti AADC (Abcam ab3905; RRID:AB_304145), anti DAT (Abcam ab5990; RRID:AB_305226), anti VMAT2 (Everest EB06558; RRID:AB_2187855), and anti β-tubulin (Sigma T4026; RRID:AB_477577). Horseradish peroxidase-coupled secondary antibodies were incubated for 1 hr at RT and signals detected and quantified after incubation in ECL with a BioRad ChemiDoc XRS + imager and Quantity One software.

2.7 | Quantification of DA, DOPAC AND HVA

Cell culture supernatant was mixed 4:1 with 2 M perchloric acid (PCA) and 1% (v/v) sodium metabisulfite (SMbS) to stabilize DA and metabolites and incubated on ice for at least 10 min. The cells were washed with PBS, and lysed in 200 μl trichloroacetic acid (TCA) per well. The cell lysate was mixed 9:1 with 2M PCA/ 1% SMbS and incubated on ice for at least 10 min. Levels of DA, DOPAC, and HVA were then determined by HPLC with electrochemical detection essentially as described (Tereshchenko, Maddalena, Bähr, & Kügler, 2014). At times of harvesting cells and supernatants, neuron numbers were counted from fluorescently labeled cells in order to allow relating DA/DOPAC/HVA amounts to numbers of neurons present in the respective culture. As such, DA, DOPAC, and HVA levels were expressed as ng/ 10^4 neurons, allowing to use the same scale for intracellular and extracellular levels from the same culture.

2.8 | NMR

Full length recombinant ^{15}N-labeled human synucleins were produced in BL21 E. coli in M9 minimal medium using $^{15}NH_4Cl$ as sole nitrogen source, purified as described (Hoyer et al., 2002) and adjusted to 100 μM final concentration in 20 mM sodium phosphate, pH 6.0, 2 mM tris-(2-carboxyethyl)phosphine (TCEP), 0.05% NaN_3, and 10% ^2H_2O. 10 mM stock solutions of DA and DOPAL were prepared in 20 mM sodium phosphate, pH 6.0, 2 mM TCEP (in order to inhibit any auto-oxidation and thus prevent artifacts like dicatechol pyrrole adducts generated by oxidized DOPAL (Werner-Allen, Levine, & Bax, 2017)) and 0.05% NaN_3. Chemical shift perturbations (CSPs) at increasing DA/DOPAL concentrations were recorded on a Bruker 800 Mhz spectrometer fitted with a CP-TCI cryoprobe. At 280K, two-dimensional ^1H - ^{15}N heteronuclear single quantum coherence (HSQC) was recorded with 100 μM synuclein and 0.02–2 mM DA and DOPAL. Because ^1H chemical shifts of intrinsically disordered proteins are extremely sensitive to changes in pH or ionic strength, which may arise as an artifact because of the addition of increasing amount of higher ligand-concentration solution into the lower ligand-concentration solution, we have focused on the ^{15}N chemical shifts as the reporter for ligand binding. However, the data were processed in multiple ways, including considering both ^1H and ^{15}N chemical shifts and exclusively ^{15}N chemical shifts, without any significant difference in results (see Figures S4 and S5). Residues were assigned according to published NMR assignments for α-Syn (Cho et al., 2009) and β-Syn (Bertoncini et al., 2007). Titration curves, with ΔδN chemical shift changes plotted versus ligand concentrations were fitted by a single binding model to obtain the dissociation constant of the interaction. Specifically, the equation.

$$\Delta = \Delta_{max}([L]_T + [P]_T + K_d - \{([L]_T + [P]_T + K_d)^2 - 4[L]_T[P]_T\}^{1/2}(2[P]_T).$$

was exploited, were $[L]_T$ is the ligand concentration, $[P]_T$ is the protein concentration, Δ_{max} is the CSP at infinite ligand concentration and K_d is the dissociation constant.

2.9 | Dopaminochrome aggregation assay

Dopaminochrome (DCH) was generated by incubation of DA with sodium periodate ($NaIO_4$)) as described (Ochs, Westfall, & Macarthur, 2005). Full length human α-Syn and β-Syn with a C-terminal 6 x His tag were expressed in E. coli and purified by Ni-NTA chromatography. Eluted proteins were dialyzed against MES/MOPS buffer (20 mM MES, 20 mM MOPS, 100 mM NaCl, pH 5.8) using 10.000 MWCO dialysis cassettes. Finally, protein concentration of the dialysed samples was adjusted to 5 mg/ml (~330μM) using MES/MOPS buffer. Two hundred microliter aliquot fractions were stored at −80°C. For fibrillation, these protein samples were incubated for 7 days at 37°C and continuous shaking at 1,000 rpm. DA and DCH were added to the reaction at equimolar concentrations to the synucleins. N-Acetyl-L-Cysteine was added at a 3-fold molar excess. DA and DCH stock solutions were prepared fresh, directly before the start of the experiment. For the thioflavin-T (Th-T) assay, α-Syn and β-Syn samples were diluted to 4.5 μM in a solution of 20 μM Th-T in PBS. This assay was conducted at pH 7.4 in order to allow for DA auto-oxidation during incubation. To promote aggregation 0.001% (w/w) of preformed β-Syn or α-Syn fibrils were added. After 7 days of incubation, the fluorescence was measured at an excitation wavelength of 440 nm and emission of 480 nm using a microplate reader (TECAN Spark). To separate between soluble and fibrillized protein, samples were centrifuged at 100,000 g for 30 min at room temperature (22°C). Pellets, containing fibrils and higher molecular weight aggregates, were resuspended in MES/MOPS

buffer. For CD measurements, the proteins were diluted in distilled water to a final concentration of 0.1 mg/ml. CD spectra of α-Syn and β-Syn samples, both monomeric and aggregated forms, were measured between 190 and 250 nm wavelength, using a 0.1 mm path quartz cuvette on a Chirascan™ CD Spectrometer.

2.10 | Statistical analysis

As no human and animal subjects were used for experimentation, the study was not pre-registered and randomized. The study was exploratory insofar because of unknown effect sizes no pre-determination of sample sizes other than that based on scientific experiences was performed. No exclusion criteria were pre-determined. Experimentation and statistical evaluation were carried out by different scientists, in a way that the evaluator received blinded data sets. Experimental data were analyzed in GraphPad Prism 8 for normal data distribution by D´Agostino-Pearson´s omnibus K2 test. Should a *single* extreme value suggested non-normal data distribution, this value was not excluded (see individual symbols in Figures 2 and 3), but the statistics was still performed

under assumption of Gaussian distribution of data, using ANOVA. In addition, the non-parametric Kruska–Wallis test with Dunn´s correction for multiple comparisons was performed, in order to confirm validity of the statistical analysis under the assumption that data were not normally distributed. For all data analyzed, ANOVA and Kruska–Wallis test delivered identical statistical outcomes. As no data points were excluded from analysis, distinct test for outliers were not performed. Thus, as shown in the figures of this study, statistically significant differences between multiple groups were evaluated by one-way ANOVA with Dunnett's post hoc test for multiple comparisons, or, in case of pairwise comparisons, by unpaired, two-tailed Student´s T-test. Bar diagrams show mean ± standard deviation (*SD*), box plots are composed according to Tukey´s (box showing Q1 to Q3 and the median, whiskers including values within 3/2 times the interquartile range of Q1 and Q3, and individual dots of outliers).

Statistical powers of all comparisons were analyzed by G*Power3.1 (Faul, Erdfelder, Buchner, & Lang, 2009) with the following settings: test family = *t*-tests (two-tailed); statistical tests = difference of means between two independent groups; type of power analysis = post hoc; effect size *d* computed from means and standard
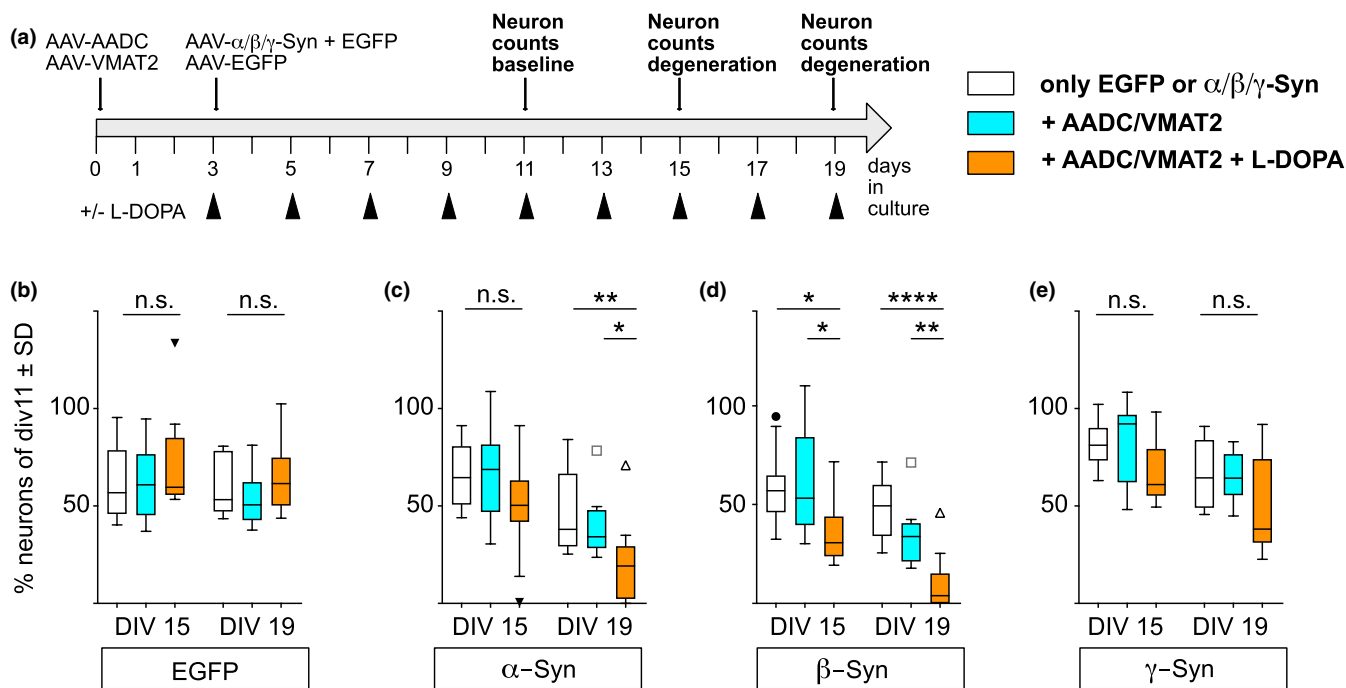
FIGURE 2 Intracellular DA synthesis enhances the neurodegenerative potential of β-Syn. (a) Schematic outline of the experimental schedule. For all conditions, neurons were counted on div 11 as a baseline value, and at div 15 and 19 to determine the ongoing neuron loss. In panels (b–e) neuron numbers are shown as percentages of neurons relative to div 11. White boxes in panels (b–e) represent neurons that were transduced only with AAVs expressing either α-Syn + EGFP, β-Syn + EGFP, γ-Syn + EGFP or EGFP alone at div3. Green boxes represent neurons that express synucleins and additionally express AADC and VMAT2 from div 0 on. Orange boxes represent neurons that express synucleins and AADC, VMAT2, and L-DOPA was added at the indicated times (triangles). (b) Percentage of surviving neurons at div 15 and div 19 in cultures expressing only EGFP. (c) Percentage of surviving neurons at div 15 and div 19 in cultures expressing α-Syn+EGFP. (d) Percentage of surviving neurons at div 15 and div 19 in cultures expressing β-Syn+EGFP. (e) Percentage of surviving neurons at div 15 and div 19 in cultures expressing γ-Syn+EGFP. Statistics by one-way ANOVA with Dunnett´s post hoc test for multiple comparisons. *$p < .05$, **$p < .01$, ****$p < .00001$; Statistical power (1-β error probability)> 0.94 for all conditions, except for * in (d), which are >0.85. $N = 11$–13 independent transductions for each condition, derived from 3 to 4 independent neuron preparations. Box plots with whiskers according to Tukey, individual outliers shown as single symbols
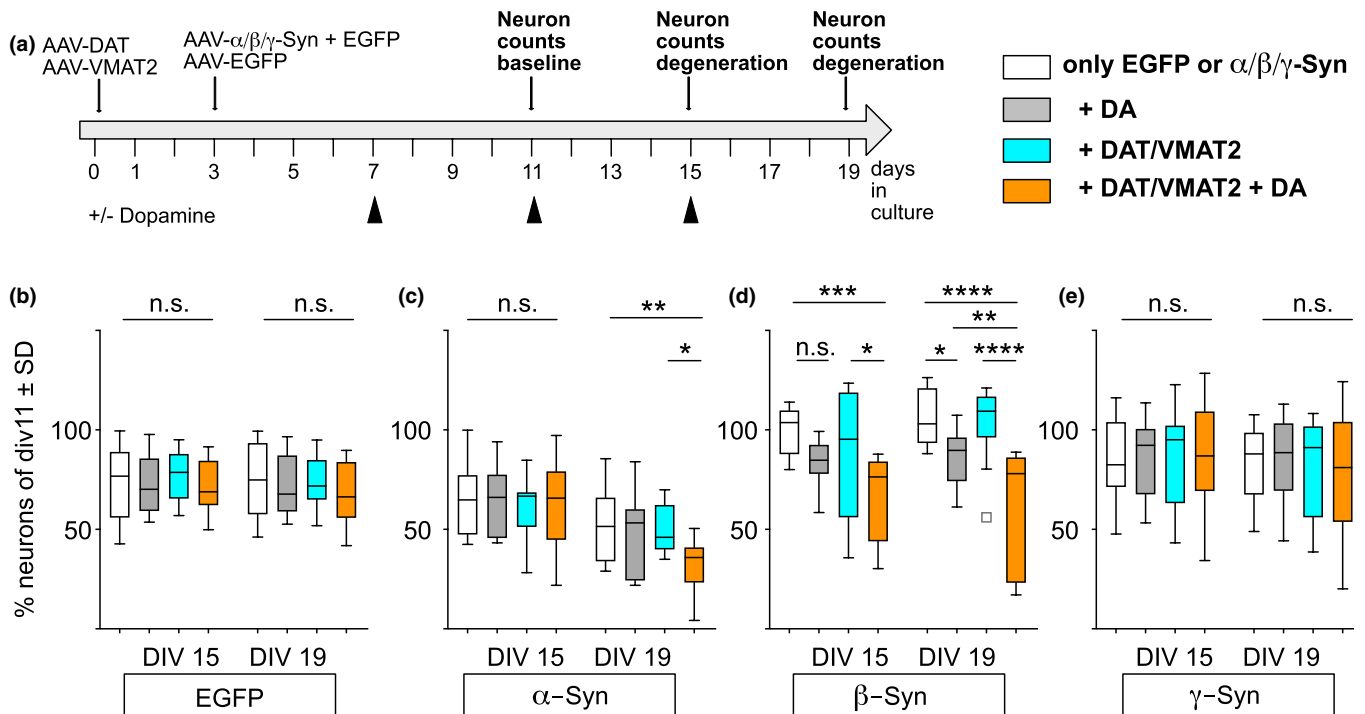
FIGURE 3 DA taken up from extracellular space enhances the neurodegenerative potential of β-Syn. (a) Schematic outline of the experimental schedule. For all conditions, neurons were counted on div 11 as a baseline value, and at div 15 and 19 to determine the ongoing neuron loss. In panels (b–e) neuron numbers are shown as percentages of neurons relative to div 11. White boxes in panels (b–e) represent neurons that were transduced only with AAVs expressing either α-Syn + EGFP, β-Syn + EGFP, γ-Syn + EGFP, or EGFP alone at div3. Grey boxes represent synuclein-expressing neurons plus addition of DA at indicated times, but without expression of DAT and VMAT2. Green boxes represent neurons that express synucleins, DAT, and VMAT2 from div 0 on, but without addition of DA. Orange boxes represent neurons that express the synucleins, DAT, and VMAT2, and DA was added at the indicated times (triangles). (b) Percentage of surviving neurons at div 15 and div 19 in cultures expressing only EGFP. (c) Percentage of surviving neurons at div 15 and div 19 in cultures expressing α-Syn+EGFP. (d) Percentage of surviving neurons at div 15 and div 19 in cultures expressing β-Syn+EGFP. (e) Percentage of surviving neurons at div 15 and div 19 in cultures expressing γ-Syn+EGFP. Statistics by one-way ANOVA with Dunnett´s post hoc test for multiple comparisons. **$p < .01$, ***$p < .001$, ****$p < .00001$; Statistical power (1-β error probability)> 0.95 for all conditions, except ** in (d), which is 0.87. $N = 11$–13 independent transductions for each condition, derived from 3 to 4 independent neuron preparations. Box plots with whiskers according to Tukey, individual outliers shown as single symbols

deviations of groups to compare; α error probability = 0.05; with given sample sizes the power of the statistical assessment was computed as (1–β error probability). A reasonable statistical power of the respective statistical analysis was assumed at (1–β error probability) >0.8.

3 | RESULTS

3.1 | Generation of a primary neuron cell culture system to study the dopamine-dependent neurotoxic potential of β-Syn

To generate neurons with a dopaminergic neurotransmitter phenotype and appropriate controls, we aimed for cells that are identical in all aspects but differ only in their capacity to synthesize or to take up DA. As a basis, we used cortical neurons isolated from embryonal rat brains. These cultures survive for long-term because of astroglial support, develop an unstimulated synchronized firing

activity (Murphy, Blatter, Wier, & Baraban, 1992) and can serve to study a wide variety of physiologic effects related to the synucleins (Tolö et al., 2018). The genuine neurotransmitter phenotype of these cells (85% are glutamatergic, 15% are GABAergic) was not erased, but persisted while adding the dopaminergic neurotransmitter phenotype. All necessary dopaminergic factors and the synucleins were expressed in these cultures by means of recombinant AAV vectors under control of a strictly neuron-specific promoter (Figure 1a–c).

Two different cultures of dopaminergic neurons were developed: intracellular dopamine synthesis was enabled by expression of aromatic amino acid decarboxylase (AADC; which converts L-DOPA into DA) and vesicular monoamine transporter 2 (VMAT2; which transports DA into synaptic vesicles), and initiated by addition of 3,4-dihydroxyphenylalanine (L-DOPA) into the cell culture medium (Figure 1d and e). Alternatively, take up and re-release of DA was enabled by expression of the dopamine transporter (DAT; which re-uptakes secreted DA from the synaptic cleft), VMAT2, and initiated by addition of DA into the cell culture supernatant (Figure 1f and g).

FIGURE 4 A dopaminergic phenotype enhances the neurotoxic potential of β-Syn in human iPSC-derived neurons. (a) Schematic depiction of the differentiation process leading to dopaminergic human neurons. (b) Schematic depiction of the differentiation process leading to glutamatergic human neurons. (c) Quantification of neurodegeneration in human neurons expressing α-Syn+EGFP, β-Syn+EGFP, γ-Syn+EGFP, or EGFP alone, either in a glutamatergic neurotransmitter phenotype (gray boxes) or a dopaminergic neurotransmitter phenotype (orange boxes), at div 40. Boxes show values from minimum to maximum, with a line representing the mean. Statistics by Student´s t-test (independent groups, 2-tailed). ** $p < .01$, n.s. = not significant; statistical power (1-β error probability) >0.9 for all conditions. $N = 9$–12 independent transductions per condition with cells derived from three independent differentiation approaches. Bars represent means $\pm$ SD

(a) Differentiation of hiPSCs into dopaminergic neurons

(b) Differentiation of hiPSCs into glutamatergic neurons

(c)
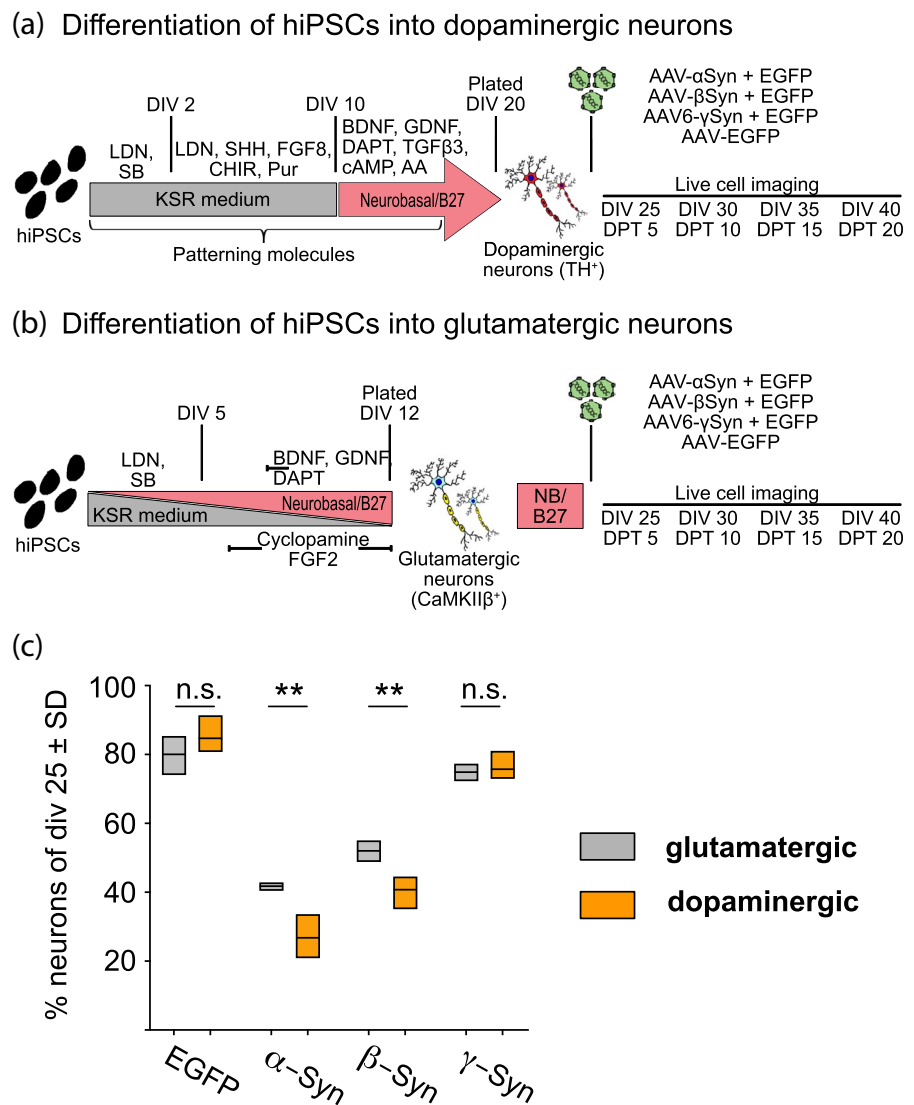
Levels of DA and its relatively stable and non-cytotoxic metabolites, 3,4-dihydroxy-phenylacetic acid (DOPAC) and homovanillic acid (HVA) that were achieved by the two strategies are shown in Figure 1e and g for cell cultures at 15 days of in vitro culture (div 15), both in cell lysates and in the cell culture supernatant. At the same time, neuron numbers were counted, and the levels of DA, DOPAC and HVA are presented as nanograms per 10.000 neurons, in order to allow for the same scale for intra- and extracellular levels.

The DA synthesis capacity of our cultures relates to that of genuine A9 dopaminergic neurons according to the following considerations: a level of 100 ng HVA/ 10.000 cultured neurons detected in supernatant of AADC/VMAT2 expressing neurons means that these cells have synthesized and released at least 100 ng of DA, which is likely to be an underestimation because of the unknown amounts of DA that became auto-oxidized. In the rat brain about 14.000 dopaminergic neurons project into the striatum, where 7–9 ng DA per 40 mg wet weight can be detected (Cheng et al., 2018), corresponding to about 200–250 ng of DA/ 10.000 neurons (i.e. 20–25 pg DA/neuron). Thus, we consider our dopaminergic neurons to be able to synthesize

DA in the same order of magnitude as genuine A9 neurons. Notably, brain synapses are much better shielded from the environment as compared to the synapses of our 2D cultures, which lose most of the synthesized DA into the cell culture supernatant because of endogenous electrical activity of the cortical neurons. Detection of intracellular DOPAC demonstrated that a certain fraction of the synthesized DA was also available for metabolism within the neuronal cytoplasm, most likely representing the activity of neuronal monoamine oxidase (MAO) and aldehyde dehydrogenase (ALDH), that catabolize DA either en route to synaptic vesicles, or degrade DA leaking from synaptic vesicles (Meiser, Weindl, & Hiller, 2013).

3.2 | Impact of a dopaminergic neurotransmitter phenotype on the neurodegenerative potential of β-Syn in primary neurons

Synuclein-induced neurodegeneration in presence or absence of DA and its metabolites was studied by expression of either α-Syn, β-Syn,

γ-Syn, or EGFP in both types of dopaminergic neuron cultures. Expression levels of the synucleins (Figure 1c) were adjusted in a way that their expression in the absence of DA caused only minor (if any) neurodegeneration on top of the normal cell loss occurring in primary cultures over time (Lesuisse & Martin, 2002). We performed baseline cell counts at div 11, in order to allow for generation of stable conditions in terms of neuronal maturation, DA production, growth of astrocytes, and establishment of endogenous network activity. Cell counts to determine ongoing neurodegeneration were then performed at div 15 and div 19, and surviving neuron numbers are presented as the percentage of cells compared to baseline counts at div 11 (Figures 2 and 3).

Figure 2 shows the impact of a dopaminergic neurotransmitter phenotype on neurons expressing EGFP, α-Syn, β-Syn, or γ-Syn for the condition in which DA is synthesized intracellularly (Figure 2a). Neurons that expressed only EGFP did not show any aggravation of neurodegeneration at div 15 or 19 because of the presence of DA (Figure 2b). Neurons that expressed α-Syn showed a moderate decline in surviving neuron numbers at div 15 when synthesizing DA, and a significant degeneration because of the presence of DA at div 19 (Figure 2c). The impact of DA synthesis on survival of β-Syn expressing neurons took place with a somewhat faster pace (Figure 2d): here, a significant cell loss because of the presence of DA was detected already at div 15, and at div 19 the majority of β-Syn expressing dopaminergic neurons had degenerated. γ-Syn expressing neurons were considered as an additional control that might be better suited as compared to EGFP, as γ-Syn did not cause evident neurotoxicity in previous studies (Taschenberger et al., 2013; Tolö et al., 2018). However, although there was no significant cell loss detected in these neurons upon DA synthesis, a trend toward reduced neuron counts was evident, suggesting that under our experimental conditions even γ-Syn might tend to develop certain neurotoxic properties in presence of DA (Figure 2e).

Figure 3 shows the impact of a dopaminergic neurotransmitter phenotype on neurons expressing EGFP, α-Syn, β-Syn, or γ-Syn for the condition in which DA is absorbed from the extracellular space (Figure 3a). Neurons that express only EGFP did not show any enhancement of neurodegeneration because of up-take of DA from the cell culture medium (Figure 3b). Neurons that express α-Syn did not show enhanced neurodegeneration because of DA up-take at div 15, but only at div 19 (Figure 3c). Neurons expressing β-Syn showed a faster progressing impact of DA on neurodegeneration: we detected a significantly enhanced neuron loss because of DA already at div 15, which was even more pronounced at div 19 (Figure 3d). In addition, β-Syn expressing neurons were the only cultures which demonstrated some neurodegeneration because of the sole presence of DA within the cell culture medium, in the absence of AADC and VMAT2 expression at div 19 ($p = .04$, power ($1-\beta$ err. prob.) $= 0.96$). If this effect is due to a low-level up-take of DA through other transport systems than DAT remains unknown. Neurons expressing γ-Syn behaved essentially as those expressing EGFP and did not present with any DA-induced aggravation of neurodegeneration (Figure 3e).

3.3 | Impact of the dopaminergic neurotransmitter phenotype on neurodegeneration induced by β-Syn in human iPSC-derived neurons

Modified primary neurons allowed to study the impact of DA on the neurotoxic potential of β-Syn in cells that were identical on the genomic level in *verum* and control conditions, but might be criticized as not having a native dopaminergic neurotransmitter phenotype. Thus, we sought to confirm our results in human iPSC-derived neurons that were differentiated into either a dopaminergic (Figure 4a) or a glutamatergic neurotransmitter phenotype (Figure 4b). Dopaminergic cultures generated in this paradigm produce DA levels detectable by HPLC with electrochemical detection only when supplied with exogenous L-DOPA. However, in absence of exogenously added L-DOPA the final metabolite HVA becomes detectable in the supernatant of these cultures at late stages (i.e.> div 35; 1.05 ± 0.6 ng/10^4 cells), demonstrating that they produce low levels of DA endogenously. It seems reasonable to speculate that this low-level DA production is due to the self-limiting control that DA exerts on TH activity (Meiser et al., 2013).

We used these cultures without addition of exogenous L-DOPA, aiming to investigate if even very low levels of DA synthesis would have detectable pathophysiological effects in combination with the synucleins. Both types of neurons were transduced with AAV vectors that co-express α-Syn, β-Syn, or γ-Syn with EGFP, or expressed EGFP alone. The number of EGFP-expressing neurons was quantified at 20 days after transduction (dpt 20, corresponding to div 40) with synuclein-expressing vectors, in order to allow for a similar time frame as used in primary neurons. Neurodegeneration induced by both α-Syn and β-Syn was moderately, but significantly aggravated in neurons of the dopaminergic neurotransmitter phenotype as compared to neurons of the glutamatergic neurotransmitter phenotype (Figure 4c). However, the effect size, that is, the difference in neurodegeneration between glutamatergic and dopaminergic neurons, was less pronounced as compared to modified rodent neurons with and without DA production, presumably because of the lower levels of DA generated by human neurons. Neurons of both neurotransmitter phenotypes showed no neurodegeneration after expression of γ-Syn or EGFP. Thus, the results obtained in human-derived neurons in principle support our findings from modified primary rat neurons, that a dopaminergic neurotransmitter phenotype promotes the neurodegenerative potential of β-Syn, even if levels of DA synthesis are low.

3.4 | Impact of β-Syn on synchronized neuronal network activity in absence and presence of DA

Besides its neurodegenerative properties, α-Syn has been shown to attenuate spontaneous synchronized network activity when overexpressed in aged cultured cortical neurons (Tolö et al., 2018). Thus, we now evaluated if β-Syn overexpression would also cause this functional defect, and if a dopaminergic neurotransmitter phenotype
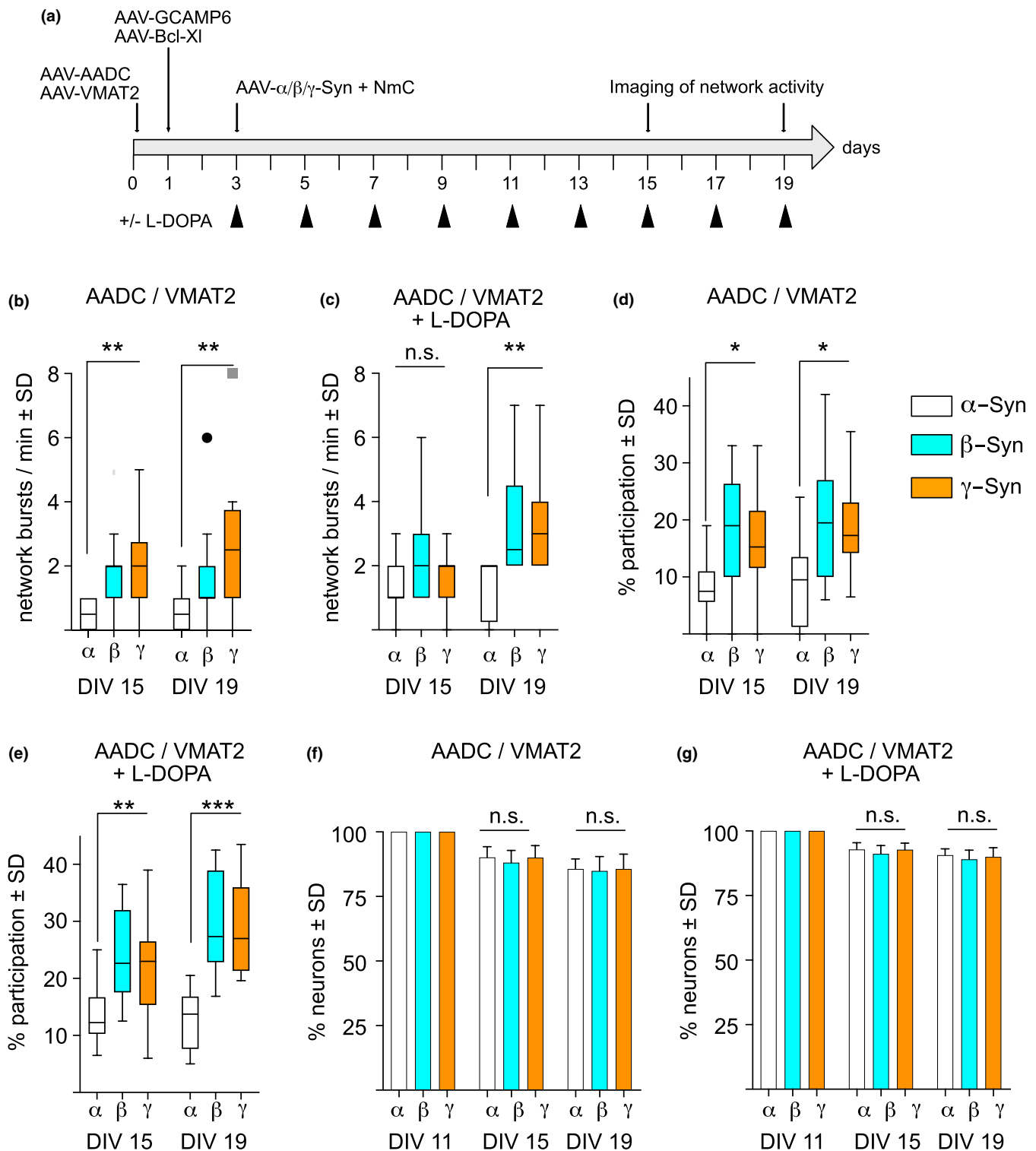
FIGURE 5 Dopamine does not cause β-Syn to impact on neuronal network activity, and its neurodegeneration-promoting effect is rescued by Bcl-XI. (a) Schematic outline of the experimental schedule. AAVs and L-DOPA were added at the times indicated by arrows or triangles. (b) Frequency of network bursts in α-Syn (white boxes), β-Syn (green boxes), or γ-Syn (orange boxes) expressing neurons without DA production. (c) Frequency of network bursts in α-Syn, β-Syn, or γ-Syn expressing neurons with DA production. (d) Percentage of neurons contributing to network activity in α-Syn, β-Syn, or γ-Syn expressing neurons without DA production. (e) Percentage of neurons contributing to network activity in α-Syn, β-Syn, or γ-Syn expressing neurons with DA production. (f) Bcl-XI-mediated survival of α-Syn, β-Syn, or γ-Syn expressing neurons in absence of DA production. (g) Bcl-XI-mediated survival of α-Syn, β-Syn, or γ-Syn expressing neurons in presence of DA production. Statistics by one-way ANOVA with Dunnett´s multiple comparisons test. *=$p < .05$; **=$p < .01$; ***=$p < .001$. Statistical power > 0.85 for all conditions. $N = 12$ measurements from 4 independently prepared neuronal cultures

FIGURE 6 Interaction of DA and DOPAL with β-Syn as determined by NMR. Titration profiles of representative residues are shown for the interaction of α-Syn and DA (a), β-Syn and DA (b), α-Syn and DOPAL (c), and β-Syn and DOPAL (d) as the extent of chemical shift perturbation (CSP) over a range of DA or DOPAL concentrations (0–700 μM for DA; 0–2000 μM for DOPAL). The k_D value shown in each diagram was calculated by a global fit considering all unambiguously identified amino-acids in α-Syn and β-Syn. Titration curves are shown for residues 20 (red), 101 (blue), 103 (green), 105 (orange) and 139 (cyan) in (a), residues 71 (red), 92 (blue), 120 (green), 129 (orange) and 132 (cyan) in (b), residues 9 (red), 31 (blue), 43 (green), 100 (orange) and 107 (cyan) in (c), and residues 18 (red), 27 (blue), 109 (green), 120 (orange), and 134 (cyan) in (d). A more detailed analysis of CSP shifts of individual amino acids, and titration profiles of individual residues under assumption of either 1:1 or 1:n fitting curves are shown in Suppl. Figures S3, S4, and S5. The sites of interaction of DA and DOPAL in α-Syn and β-Syn are shown as CSP intensities against the amino-acid sequence for α-Syn and DA (e), β-Syn and DA (f), α-Syn and DOPAL (g), and β-Syn and DOPAL (h). CSPs were recorded at DA and DOPAL concentration of 500 μM. The position of the ^{125}YEMPS^{129} sequence in α-Syn and the corresponding sequence ^{118}YEDPP^{122} in β-Syn are outlined in (e and f). Amino acids with outstanding CSPs in β-Syn and their corresponding residues in α-Syn are outlined in (g and h)

would have any aggravating effect in this regard. We compared spontaneous synchronized activity in primary cortical neurons that overexpressed α-Syn, β-Syn, or γ-Syn, either in unmodified neurons or in neurons provided with a dopaminergic neurotransmitter phenotype by AADC and VMAT2 expression and supplied with L-DOPA. All cultures also expressed the genetically encoded calcium sensor GCaMP6 to record network activity, and in addition the anti-apoptotic factor Bcl-Xl, which had been shown to protect primary neurons from neurodegeneration by preventing synuclein-induced damage of the outer mitochondrial membrane in absence of DA (Tolö et al., 2018) (Figure 5a). If Bcl-Xl would prevent neurodegeneration in presence of DA, this would be indicative for DA enhancing mitochondrial outer membrane damage.

In the absence of DA α-Syn expressing cultures showed a reduced spontaneous burst frequency (Figure 5b) and a reduced number of neurons participating in this activity (Figure 5d), as compared to controls expressing γ-Syn, which behave equal to native neurons (Tolö et al., 2018). The presence of DA significantly enhanced the synchronized burst frequency of α-Syn expressing cultures (without DA: 0.5 ± 0.5 bursts/min, with DA: 1.4 ± 0.9 bursts/min; mean $\pm$ *SD*, $p = .006$; unpaired, two-tailed *t*-test) (Figure 5b versus 5c). In contrast to α-Syn expressing cultures, β-Syn expressing cultures did not show significantly reduced network activity as compared to controls in absence of DA (Figure 5b), and also no diminishment of neurons contributing to this activity (Figure 5d). Again, presence of DA rather enhanced than reduced neuronal activity in β-Syn expressing cultures (Figure 5c and e).

3.5 | Protection of mitochondrial outer membrane integrity prevents the neuropathological impact of β-Syn and DA

No confounding effect on network activity through neurodegeneration was detectable in this experiment, as Bcl-Xl expression kept neuron numbers constant in both absence (Figure 5f) and presence of DA (Figure 5g).Thus, our current data show that Bcl-Xl was able to provide the same full neuroprotection against α-Syn and β-Syn in DA producing neurons as compared to non-DA producing neurons, suggesting that DA promotes the neurotoxic potentials of both α-Syn and β-Syn by a mechanism that depends at least to a

significant extent on damaging the integrity of the outer mitochondrial membrane.

3.6 | Interaction of β-Syn with DA

Given that DA promoted the neurotoxic potential of β-Syn, we next asked the question if this could be because of a direct interaction of DA with β-Syn. Therefore, we used NMR to investigate the interaction of β-Syn with DA and its metabolite DOPAL. This metabolite was chosen since (1) DOPAL was demonstrated to be directly neurotoxic to nigral dopaminergic neurons (Burke et al., 2008) and (2) DOPAL is produced by MAO at the outer mitochondrial membrane (Meiser et al., 2013), a sub-cellular location with high vulnerability for synuclein toxicity (Tolö et al., 2018). For comparison, interaction of α-Syn with DA and DOPAL was investigated under identical conditions. Experiments were carried out in solution containing a strong anti-oxidant in order to prevent auto-oxidation of DA or DOPAL. Experimental conditions were chosen to maintain the synucleins within a monomeric state, which was proven by absence of chemical shift perturbation (CSP) intensity decline over the time course of the measurements, indicating that no monomers have been consumed into oligomers or aggregates. The intensity of the protein NMR peaks was monitored throughout the experiments to rule out any time dependent depletion of monomer species.

The dissociation constant (k_D) for DA and β-Syn was determined to be 866 ± 98 μM, as compared to 96 ± 75 μM for DA and α-Syn (Figure 6a and b). For the interaction of DOPAL with the synucleins we determined k_Ds of 170 ± 37 μM for β-Syn, and > 3 mM for α-Syn (Figure 6c and d). These data demonstrate that DA and DOPAL show a highly divergent interaction potential with either β-Syn or α-Syn, in that DA has a 10-fold higher affinity for α-Syn, while DOPAL has a more than 10-fold higher affinity for β-Syn. While none of these k_D values suggest an ultra-high affinity between synucleins and DA or metabolites of DA, they are still in a physiological relevant range, given the high intracellular concentrations of synucleins and DA (see Discussion).

For α-Syn, we found that DA interacted predominantly with all amino acids in the C-terminus of the protein (Figure 6e), including but clearly extending the ^{125}YEMPS^{129} motif considered important for the DA-mediated inhibition of α-Syn fibrillation (Herrera
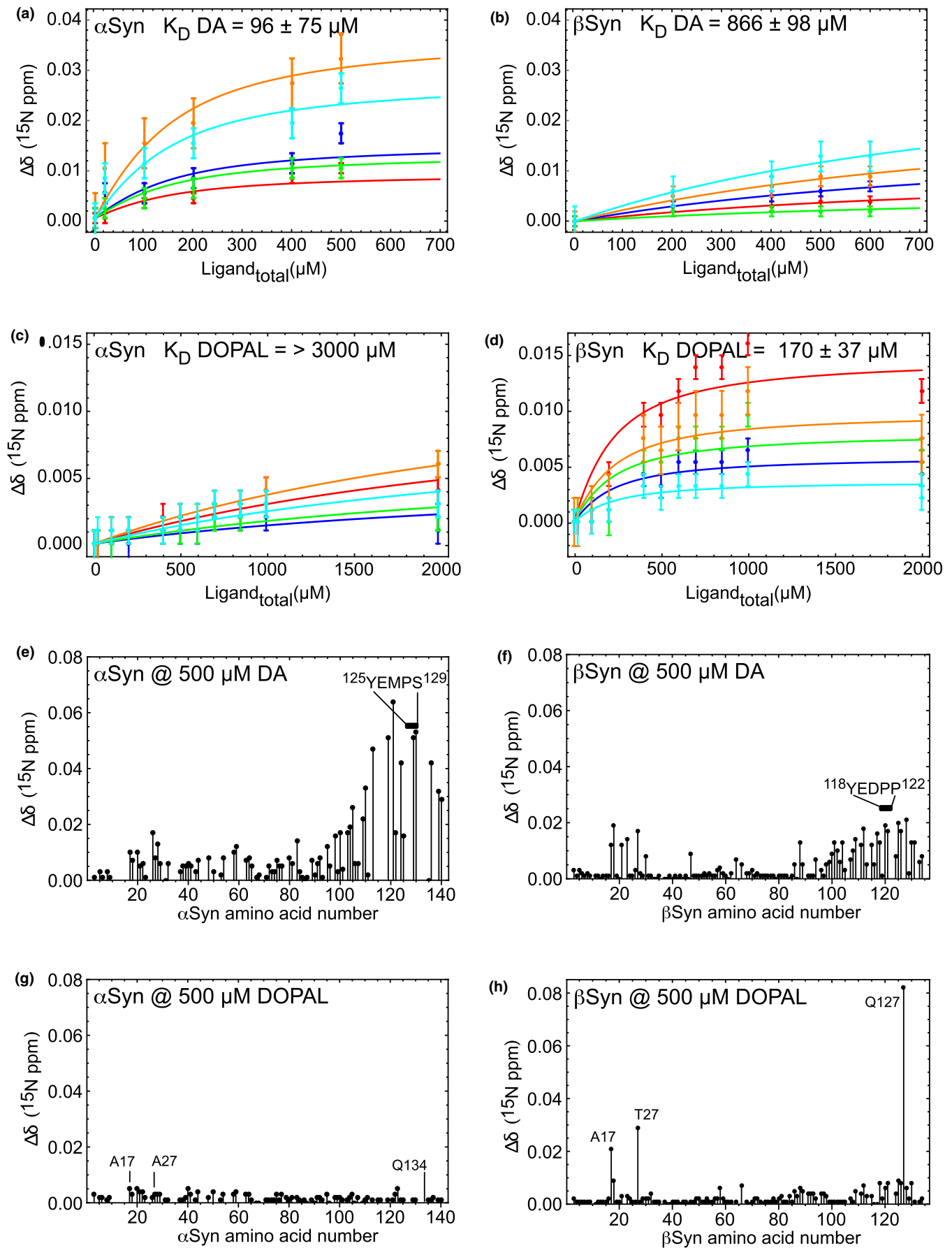
et al., 2008). For β-Syn a similar tendency was obtained, although with an about 3-fold lower affinity for C-terminal amino acid residues (Figure 6f). DOPAL interacted specifically with two amino acids in the N-terminus of β-Syn (A17 and T27), but its interaction with the corresponding amino acids of α-Syn was substantially weaker (Figure 6g). Since residue 27 is A in α-Syn but T in β-Syn, this finding suggests that individual amino acids that are not conserved between both synucleins may indeed alter the affinity for ligands such as DOPAL. Furthermore, DOPAL induced the biggest chemical shift change on Q127 in the C-terminus of β-Syn (Figure 6h). Unfortunately, the spectrum of Q134, the corresponding amino acid of α-Syn, was consistently overlapped, making it impossible to assign a CSP value to this residue.

## 3.7 | Fibrillation of β-Syn is inhibited by the oxidized DA metabolite dopaminochrome (DCH)

Finally, we investigated if DA and/or oxidized metabolites could modify the aggregation properties of β-Syn. We incubated β-Syn under conditions allowing it to form fibrils in vitro, with either DA, DA plus the antioxidant N-acetyl-cysteine (Nac) or with the oxidized metabolite dopaminochrome (DCH), and recorded fibril formation by the thioflavin-T (Th-T) assay. DCH was chosen as an oxidized metabolite because it is able to inhibit fibrillation of α-Syn (Norris et al., 2005) and is directly neurotoxic to nigral dopaminergic neurons (Touchette, Breckenridge, Wilken, & Macarthur, 2016). Our data demonstrate that incubation with DA partially inhibited fibrillation of β-Syn, most likely because of the partial oxidation of DA during the incubation process. When this oxidation of DA was prevented by Nac, β-Syn fibrillation was promoted as compared to incubation with DA alone. In contrast, incubation of β-Syn with DCH almost completely prevented fibrillation of β-Syn (Figure 7a). These findings were almost identical to those obtained for incubation of α-Syn with DA, DA + Nac, or DCH (Figure 7b). Thus, neurotoxic metabolites of DA can interact with β-Syn in the same principal way as with α-Syn, in that they prevent formation of protein fibrils and potentially enhance the concentration of toxic oligomers. At the endpoint of the aggregation assay fibrillar components were pelleted by centrifugation, and were analyzed for secondary structure elements alongside the soluble protein fractions by circular dichroism (CD). These analyses confirmed that the soluble protein fractions under all conditions present with a predominant random coiled secondary structure, as demonstrated by the minimum close to 200 nm in molar residue ellipticity (MRE) (Figure 7c–f, solid lines). In contrast, the pellet fraction contained predominately β-sheet rich secondary structures (MRE maximum at 200 nm, MRE minimum at 225 nm; dashed lines in Figure 7c–e), except for samples derived from incubation of β-Syn with DCH, which did not contain any proteinaceous components with defined secondary structure (dashed line in Figure 7f). These results obtained by end-point analysis of the aggregation assay were confirmed by analysis of early fibrillation kinetics, analysis of protein species in pellet and supernatant of the sedimentation assay and by electron microscopy (Figure S7).

4 | DISCUSSION

Our data demonstrate that β-Syn can substitute for α-Syn in an aspect that is considered central for the etiology of PD, that is, the selective vulnerability of dopaminergic neurons for neurodegeneration. Several studies have already suggested that DA and α-Syn act cooperatively as culprits in models of PD (Alvarez-Fischer et al., 2008; Mor et al., 2017, 2019; Mosharov, Larsen, & Kanter, 2009; Ulusoy, Björklund, Buck, & Kirik, 2012; Xu et al., 2002), but no such evidence was available for β-Syn up to now. Our recent finding that β-Syn can aggregate in dopaminergic neurons of the rat substantia nigra in vivo, and causes neurodegeneration in these neurons to similar extent as compared to α-Syn, already indicated that β-Syn has a neuropathological potential very similar to that of α-Syn (Taschenberger et al., 2013). However, this resemblance was also found in cultured non-dopaminergic neurons (Taschenberger et al., 2013; Tolö et al., 2018), and thus the relative impact of the dopaminergic neurotransmitter phenotype was elusive so far. Our current results obtained in three independent cell culture models now clearly demonstrate that β-Syn and α-Syn possess an almost identical neuropathological profile in terms of potentiation of neurodegeneration through a dopaminergic neurotransmitter phenotype. The fact that β-Syn has not yet been detected in Lewy bodies (Shults, 2006; Spillantini & Goedert, 2018; Spillantini et al., 1997) does not contradict an important contribution of β-Syn to etiology of PD, given that not fibrils, but oligomers are considered to be the major neurotoxic entities in synucleinopathies (Karpinar, Balija, & Kügler, 2009; Rockenstein, Nuber, & Overk, 2014). Thus, while substantial amounts of α-Syn might be sequestered in Lewy bodies to render them nontoxic, it might be that β-Syn persists within the cytoplasm as more or less soluble oligomers, which might cause, for example, mitochondrial lesions as described (Tolö et al., 2018). Therefore, future modeling of synucleinopathies should consider both α-Syn and β-Syn as potential culprits, and probably neuropathological impacts of one synuclein cannot be considered independently from the other synuclein.

With respect to the physical interaction of DA and its oxidized, neurotoxic metabolites with β-Syn we describe both commonalities and differences to α-Syn: the inhibition of β-Syn`s aggregation by DCH demonstrates that the functional interaction of oxidized DA metabolites with β-Syn follows the same principal pathway as for α-Syn. In solution and in the absence of seeds, β-Syn forms fibrils only at slightly acidic pH of 5.8, which can be taken representative for the endocytic and secretory compartments of cells (late endosomes, Golgi, secretory, and synaptic vesicles) (Demaurex, 2002). A slightly acidic environment can also be found in the intermembrane space of mitochondria, where proton traps inside cristae microdomains might generate a pH significantly below 7 even under normal physiological conditions (Santo-Domingo & Demaurex, 2012). The fact that β-Syn forms proteinase K-resistant fibrils in dopaminergic neurons in vivo illustrates that it can also aggregate in a cellular environment (Taschenberger et al., 2013). Thus, our data show that the aggregation state of β-Syn can be modified by oxidized metabolites of DA, resulting in formation of potentially more neurotoxic oligomeric species.
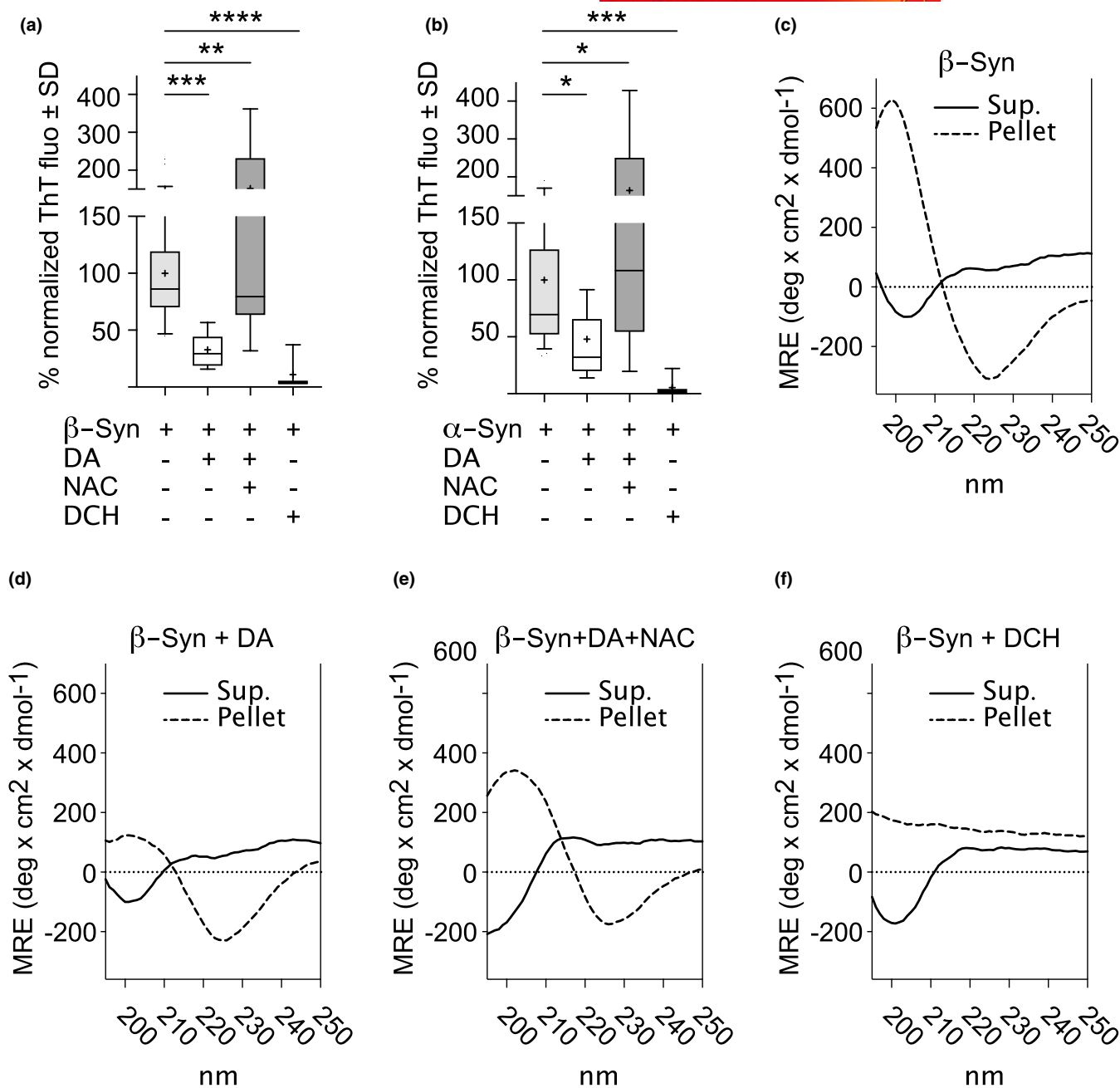
FIGURE 7 Oxidized DA metabolite dopaminochrome (DCH) inhibits fibrillation of β-Syn. (a) Thioflavin -T (ThT) incorporation into β-sheet rich structures was determined for β-Syn alone or in combination with DA, with DA+Nac, or with DCH. (b) ThT incorporation determined for α-Syn alone or in combination with DA, with DA+Nac, or with DCH. Boxes of box plots comprise the 25%–75% percentiles, whiskers show values within 10%–90% percentiles. A line within boxes denotes the median, a cross within boxes denotes the mean. To allow for the same scale in (a) and (b), ThT signal intensities obtained for β-Syn or α-Syn alone were set as 100%, respectively, and all other values were put in proportion. Kinetic raw data are depicted in more detail in Figure S7. (c) Circular dichroism (CD) spectra generated from soluble (solid lines) and pelleted (dashed line) protein derived from aggregation of β-Syn alone. (d) CD spectra generated from soluble and pelleted protein derived from aggregation of β-Syn + DA. (e) CD spectra generated from soluble and pelleted protein derived from aggregation of β-Syn + DA +Nac. (f) CD spectra generated from soluble and pelleted protein derived from aggregation of β-Syn + DCH. Statistics by one-way ANOVA with Dunnett´s multiple comparisons test. *=$p < .05$; **=$p < .01$; ***=$p < .001$; ****=$p < .0001$. Statistical power > 0.95 for all conditions except for the difference between synucleins alone and synucleins incubated with DA + Nac, which is 0.65 in (a) and (b). $N = 12$ measurements from four independent assays, with protein derived from two independent preparations

However, the precise nature of the oligomeric/aggregates species of β-Syn generated under influence of DA in a cellular context remain to be evaluated.

Differences between interactions of the two synucleins with DA and metabolites of DA were evident as well. The k_ds determined for interaction of β-Syn with DA and DOPAL vary by almost

one order of magnitude from those determined for α-Syn and DA/DOPAL. Interestingly, β-Syn has a much higher affinity for DOPAL and a much lower affinity for DA as compared to α-Syn. It remains to be determined if further oxidized metabolites of DA such as dopamine-o-quinone (Asanuma et al., 2003), 5,6-Dihydroxyindole (Pham et al., 2009), Indole-5,6-quinone (Bisaglia, Mammi, & Bubacco, 2007), or salsolinol (do Carmo-Goncalves, 2018), are also interacting with β-Syn and α-Syn with significantly different affinities. If this would be the case, then not only the levels of oxidized metabolites of DA and of the synucleins may be important for the etiology of synucleinopathies, but also cellular conditions which favor generation of the one over the other metabolite of DA.

Dissociation constants for the synucleins and DA/DOPAL were found to be in the higher micromolar range, and thus comparable to k_Ds that were found for the interaction of α-Syn with metal ions like copper (Miotto, Binolfi, Zweckstetter, Griesinger, & Fernandez, 2014). These k_Ds are orders of magnitude higher than those of high affinity interactions with immediate biological relevance, for example the binding of steroids to plasma carrier proteins or interactions of pro- and anti-apoptotic proteins, with k_Ds that are in the range of 1–10 nM (Zheng, Viacava Follis, Kriwacki, & Moldoveanu, 2016). None the less, given the high concentrations of DA within dopaminergic neurons and the high levels of β-Syn and α-Syn especially at synaptic sites, biologically relevant interactions are still very likely. Assuming that about 50% of a typical neuronal volume of 6 pl (Healy-Stoffel, Ahmad, Stanford, & Levant, 2012; Hosseini-Sharifabad & Nyengaard, 2007; Howard et al., 1993) is available for cytoplasmic distribution of DA and metabolites, 20 pg DA/neuron corresponds to a concentration of 43 mM. The majority of DA is sequestered within synaptic vesicles, reaching concentrations up to 300 mM (Pothos, Davila, & Sulzer, 1998). However, only 1% of the intracellular DA that would not be sequestered in vesicles but be available for interaction with synucleins, still represents a cytoplasmic concentration of about 400 μM. For levels of the synucleins, we consider cellular concentrations of about 300 μM after overexpression and about 60 μM for endogenous levels. This was deduced from western blots as shown in Figure 1c, where the protein equivalent of 4000–5000 neurons, corresponding to a cytoplasmic volume of 12 nl, was loaded alongside known amounts of recombinant synucleins. These calculations suggest that k_Ds in the higher micromolar range for the interaction of DA or metabolites of DA with the synucleins are clearly physiologically relevant.

Alternatively, or probably additionally, the aggravated pace of neurodegeneration caused by β-Syn and α-Syn in the dopaminergic neurotransmitter phenotype might depend on damage of neurons through the enhanced oxidative burden because of DA catabolism, which generates considerable amounts of reactive oxygen species (ROS). Primarily, hydrogen peroxide is produced as a by-product of MAO-mediated oxidative deamination of DA at the outer mitochondrial membrane (OMM) (Meiser et al., 2013). Recent studies in primary neurons have revealed that α-Syn overabundance amplifies the oxidative burden within mitochondria, and that degeneration of β-Syn and α-Syn expressing neurons eventually proceeds because of

damage of the OMM (Tolö et al., 2018). Considering DA metabolism as an additional oxidative stressor that might attack integrity of mitochondrial membrane components, it seems likely that this additive attack results in faster or more pronounced neuronal death, probably even independent from synuclein oligomerization or aggregation. The fact that Bcl-Xl, the major watchdog of OMM integrity, was able to prevent neurodegeneration caused by the combined activity of α-Syn and β-Syn expression and dopaminergic metabolism, argues in favor of this line of interpretation. Nonetheless, ROS production and synuclein oligomerization may both converge their detrimental impact on the outer mitochondrial membrane, thereby suggesting a reasonable mechanism of how the dopaminergic neurotransmitter phenotype might aggravate the neurotoxic potential of β-Syn.

5 | CONCLUSION

In conclusion, we have demonstrated that a dopaminergic neurotransmitter phenotype robustly promotes the neurodegenerative potential of β-Syn, supporting the hypothesis that β-Syn can act as a neurodegenerative culprit specifically in dopaminergic neurons. We also show that β-Syn physically interacts with DA and neurotoxic metabolites of DA, which can affect the aggregation propensities of β-Syn. Thus, it seems warranted to reconsider the role of β-Syn in the etiology of synucleinopathies like PD and DLB, at least when it comes to the influence of β-Syn on degeneration of dopaminergic neurons.

6 | COMPETING INTERESTS

The authors declare that they have no competing interests. Mathias Bähr serves as an Editor for the Journal of Neurochemistry.

7 | AUTHORS' CONTRIBUTIONS (ACCORDING TO CREDIT TAXONOMY)

AR, KL, SG, SUM, and KSC contributed to investigation, methodology, formal analysis, and visualization. DV contributed to Investigation, formal analysis, and visualization. SB contributed to resources. CG contributed to resources, conceptualization, supervision, validation, and funding acquisition. MB contributed to resources, funding acquisition, and supervision. SK contributed to conceptualization, supervision, validation, funding acquisition, visualization, and writing. All authors discussed and approved the manuscript.

All experiments were conducted in compliance with the ARRIVE guidelines.

OPEN RESEARCH BADGES

This article has received a badge for *Open Materials* because it provided all relevant information to reproduce the study in the manuscript. More information about the Open Science badges can be found at https://cos.io/our-services/open-science-badges/.

DATA AVAILABILITY STATEMENT

All data generated or analyzed during this study are included in this published article.

ORCID

Anupam Raina https://orcid.org/0000-0001-9995-9219
Sebastian Kügler https://orcid.org/0000-0002-5130-2012

REFERENCES

Alvarez-Fischer, D., Henze, C., Strenzke, C., Westrich, J., Ferger, B., Hoglinger, G. U., ... Hartmann, A. (2008). Characterization of the striatal 6-OHDA model of Parkinson's disease in wild type and alpha-synuclein-deleted mice. *Experimental Neurology*, *210*, 182–193.

Asanuma, M., Miyazaki, I., & Ogawa, N. (2003). Dopamine- or L-DOPA-induced neurotoxicity: The role of dopamine quinone formation and tyrosinase in a model of Parkinson's disease. *Neurotoxicity Research*, *5*, 165–176. https://doi.org/10.1007/BF03033137

Bertoncini, C. W., Rasia, R. M., Lamberto, G. R., Binolfi, A., Zweckstetter, M., Griesinger, C., & Fernandez, C. O. (2007). Structural characterization of the intrinsically unfolded protein beta-synuclein, a natural negative regulator of alpha-synuclein aggregation. *Journal of Molecular Biology*, *372*, 708–722.

Bisaglia, M., Mammi, S., & Bubacco, L. (2007). Kinetic and structural analysis of the early oxidation products of dopamine: Analysis of the interactions with alpha-synuclein. *Journal of Biological Chemistry*, *282*, 15597–15605. https://doi.org/10.1074/jbc.M610893200

Brown, J. W. P., Meisl, G., Knowles, T. P. J., Buell, A. K., Dobson, C. M., & Galvagnion, C. (2018). Kinetic barriers to alpha-synuclein protofilament formation and conversion into mature fibrils. *Chemical Communications (Cambridge, England)*, *54*, 7854–7857.

Burke, W. J., Kumar, V. B., Pandey, N., Panneton, W. M., Gan, Q., Franko, M. W., ... Galvin, J. E. (2008). Aggregation of alpha-synuclein by DOPAL, the monoamine oxidase metabolite of dopamine. *Acta Neuropathologica*, *115*, 193–203.

Cappai, R., Leck, S. L., Tew, D. J., Williamson, N. A., Smith, D. P., Galatis, D., ... Hill, A. F. (2005). Dopamine promotes alpha-synuclein aggregation into SDS-resistant soluble oligomers via a distinct folding pathway. *The FASEB Journal*, *19*, 1377–1379.

Cheng, S., Tereshchenko, J., Zimmer, V., Vachey, G., Pythoud, C., Rey, M., ... Kügler, S. (2018). Therapeutic efficacy of regulable GDNF expression for Huntington's and Parkinson's disease by a high-induction, background-free "GeneSwitch" vector. *Experimental Neurology*, *309*, 79–90. https://doi.org/10.1016/j.expneurol.2018.07.017

Cho, M. K., Nodet, G., Kim, H. Y., Jensen, M. R., Bernado, P., Fernandez, C. O., ... Zweckstetter, M. (2009). Structural characterization of alpha-synuclein in an aggregation prone state. *Protein Science*, *18*, 1840–1846.

Demaurex, N. (2002). pH Homeostasis of cellular organelles. *News in Physiological Sciences*, *17*, 1–5. https://doi.org/10.1152/physiologyonline.2002.17.1.1

do Carmo-Goncalves, P., Coelho-Cerqueira, E., & Cortines, J. R., de Souza, T. L. F., Romao, L., & Follmer, C. (2018). In vitro neurotoxicity of salsolinol is attenuated by the presynaptic protein alpha-synuclein. *Biochimica Et Biophysica Acta - General Subjects*, *1862*, 2835–2845.

Espay, A. J., Vizcarra, J. A., Marsili, L., Lang, A. E., Simon, D. K., Merola, A., ... Leverenz, J. B. (2019). Revisiting protein aggregation as pathogenic in sporadic Parkinson and Alzheimer diseases. *Neurology*, *92*, 329–337. https://doi.org/10.1212/WNL.0000000000006926

Fan, Y., Limprasert, P., Murray, I. V., Smith, A. C., Lee, V. M., Trojanowski, J. Q., ... La Spada, A. R. (2006). Beta-synuclein modulates alpha-synuclein neurotoxicity by reducing alpha-synuclein protein expression. *Human Molecular Genetics*, *15*, 3002–3011.

Faul, F., Erdfelder, E., Buchner, A., & Lang, A. G. (2009). Statistical power analyses using G*Power 3.1: Tests for correlation and regression analyses. *Behavior Research Methods*, *41*, 1149–1160. https://doi.org/10.3758/BRM.41.4.1149

Galvin, J. E., Lee, V. M., & Trojanowski, J. Q. (2001). Synucleinopathies: Clinical and pathological implications. *Archives of Neurology*, *58*, 186–190. https://doi.org/10.1001/archneur.58.2.186

Giasson, B. I., Murray, I. V., Trojanowski, J. Q., & Lee, V. M. (2001). A hydrophobic stretch of 12 amino acid residues in the middle of alpha-synuclein is essential for filament assembly. *Journal of Biological Chemistry*, *276*, 2380–2386.

Hashimoto, M., Rockenstein, E., Mante, M., Crews, L., Bar-On, P., Gage, F. H., ... Masliah, E. (2004). An antiaggregation gene therapy strategy for Lewy body disease utilizing beta-synuclein lentivirus in a transgenic model. *Gene Therapy*, *11*, 1713–1723.

Healy-Stoffel, M., Ahmad, S. O., Stanford, J. A., & Levant, B. (2012). A novel use of combined tyrosine hydroxylase and silver nucleolar staining to determine the effects of a unilateral intrastriatal 6-hydroxydopamine lesion in the substantia nigra: A stereological study. *Journal of Neuroscience Methods*, *210*, 187–194. https://doi.org/10.1016/j.jneumeth.2012.07.013

Herrera, F. E., Chesi, A., Paleologou, K. E., Schmid, A., Munoz, A., Vendruscolo, M., ... Carloni, P. (2008). Inhibition of alpha-synuclein fibrillization by dopamine is mediated by interactions with five C-terminal residues and with E83 in the NAC region. *PLoS One*, *3*, e3394.

Hosseini-Sharifabad, M., & Nyengaard, J. R. (2007). Design-based estimation of neuronal number and individual neuronal volume in the rat hippocampus. *Journal of Neuroscience Methods*, *162*, 206–214. https://doi.org/10.1016/j.jneumeth.2007.01.009

Howard, C. V., Jolleys, G., Stacey, D., Fowler, A., Wallen, P., & Browne, M. A. (1993). Measurement of total neuronal volume, surface area, and dendritic length following intracellular physiological recording. *Neuroprotocols*, *2*(2), 113–120. https://doi.org/10.1006/ncmn.1993.1016

Hoyer, W., Antony, T., Cherny, D., Heim, G., Jovin, T. M., & Subramaniam, V. (2002). Dependence of alpha-synuclein aggregate morphology on solution conditions. *Journal of Molecular Biology*, *322*, 383–393.

Jinsmaa, Y., Sharabi, Y., Sullivan, P., Isonaka, R., & Goldstein, D. S. (2018). 3,4-Dihydroxyphenylacetaldehyde-Induced Protein Modifications and Their Mitigation by N-Acetylcysteine. *Journal of Pharmacology and Experimental Therapeutics*, *366*, 113–124.

Karpinar, D. P., Balija, M. B., Kügler, S., Opazo, F., Rezaei-Ghaleh, N., Wender, N., ... Zweckstetter, M. (2009). Pre-fibrillar alpha-synuclein variants with impaired beta-structure increase neurotoxicity in Parkinson's disease models. *EMBO Journal*, *28*, 3256–3268.

Kasten, M., & Klein, C. (2013). The many faces of alpha-synuclein mutations. *Movement Disorders*, *28*, 697–701. https://doi.org/10.1002/mds.25499

Kriks, S., Shim, J.-W., Piao, J., Ganat, Y. M., Wakeman, D. R., Xie, Z., … Studer, L. (2011). Dopamine neurons derived from human ES cells efficiently engraft in animal models of Parkinson's disease. *Nature*, *480*, 547–551. https://doi.org/10.1038/nature10648

Kügler, S., Lingor, P., Schöll, U., Zolotukhin, S., & Bähr, M. (2003). Differential transgene expression in brain cells in vivo and in vitro from AAV-2 vectors with small transcriptional control units. *Virology*, *311*, 89–95. https://doi.org/10.1016/S0042-6822(03)00162-4

Lesuisse, C., & Martin, L. J. (2002). Long-term culture of mouse cortical neurons as a model for neuronal development, aging, and death. *Journal of Neurobiology*, *51*, 9–23. https://doi.org/10.1002/neu.10037

Mahajani, S., Raina, A., Fokken, C., Kügler, S., & Bähr, M. (2019). Homogenous generation of dopaminergic neurons from multiple hiPSC lines by transient expression of transcription factors. *Cell Death & Disease*, *10*, 898. https://doi.org/10.1038/s41419-019-2133-9

Meiser, J., Weindl, D., & Hiller, K. (2013). Complexity of dopamine metabolism. *Cell Communication and Signaling*, *11*, 34. https://doi.org/10.1186/1478-811X-11-34

Miotto, M. C., Binolfi, A., Zweckstetter, M., Griesinger, C., & Fernandez, C. O. (2014). Bioinorganic chemistry of synucleinopathies: Deciphering the binding features of Met motifs and His-50 in AS-Cu(I) interactions. *Journal of Inorganic Biochemistry*, *141*, 208–211. https://doi.org/10.1016/j.jinorgbio.2014.08.012

Mor, D. E., Daniels, M. J., & Ischiropoulos, H. (2019). The usual suspects, dopamine and alpha-synuclein, conspire to cause neurodegeneration. *Movement Disorders: Official Journal of the Movement Disorder Society*, *34*, 167–179. https://doi.org/10.1002/mds.27607

Mor, D. E., Tsika, E., Mazzulli, J. R., Gould, N. S., Kim, H., Danielsm, M. J., … Ischiropoulos, H. (2017). Dopamine induces soluble alpha-synuclein oligomers and nigrostriatal degeneration. *Nature Neuroscience*, *20*, 1560.

Moriarty, G. M., Olson, M. P., Atieh, T. B., Janowska, M. K., Khare, S. D., & Baum, J. (2017). A pH-dependent switch promotes beta-synuclein fibril formation via glutamate residues. *Journal of Biological Chemistry*, *292*, 16368–16379.

Mosharov, E. V., Larsen, K. E., Kanter, E., Phillips, K. A., Wilson, K., Schmitz, Y., & Sulzer, D. (2009). Interplay between cytosolic dopamine, calcium, and alpha-synuclein causes selective death of substantia nigra neurons. *Neuron*, *62*, 218–229.

Murphy, T. H., Blatter, L. A., Wier, W. G., & Baraban, J. M. (1992). Spontaneous synchronous synaptic calcium transients in cultured cortical neurons. *Journal of Neuroscience*, *12*, 4834–4845. https://doi.org/10.1523/JNEUROSCI.12-12-04834.1992

Norris, E. H., Giasson, B. I., Hodara, R., Xu, S., Trojanowski, J. Q., Ischiropoulos, H., & Lee, V. M. (2005). Reversible inhibition of alpha-synuclein fibrillization by dopaminochrome-mediated conformational alterations. *Journal of Biological Chemistry*, *280*, 21212–21219.

Ochs, S. D., Westfall, T. C., & Macarthur, H. (2005). The separation and quantification of aminochromes using high-pressure liquid chromatography with electrochemical detection. *Journal of Neuroscience Methods*, *142*, 201–208. https://doi.org/10.1016/j.jneumeth.2004.08.010

Park, J. Y., & Lansbury, P. T. Jr (2003). Beta-synuclein inhibits formation of alpha-synuclein protofibrils: A possible therapeutic strategy against Parkinson's disease. *Biochemistry*, *42*, 3696–3700.

Pham, C. L., Leong, S. L., Ali, F. E., Kenche, V. B., Hill, A. F., Gras, S. L., … Cappai, R. (2009). Dopamine and the dopamine oxidation product 5,6-dihydroxylindole promote distinct on-pathway and off-pathway aggregation of alpha-synuclein in a pH-dependent manner. *Journal of Molecular Biology*, *387*, 771–785.

Phansalkar, N., More, S., Sabale, A., & Joshi, M. (2011). Adaptive local thresholding for detection of nuclei in diversity stained cytology images (pp. 218–220). IEEE. In: 2011 International Conference on Communications and Signal Processing

Planchard, M. S., Exley, S. E., Morgan, S. E., & Rangachari, V. (2014). Dopamine-induced alpha-synuclein oligomers show self- and cross-propagation properties. *Protein Science*, *23*, 1369–1379.

Poewe, W., Seppi, K., Tanner, C. M., Halliday, G. M., Brundin, P., Volkmann, J., … Lang, A. E. (2017). Parkinson disease. *Nature Reviews Disease Primers*, *3*. https://doi.org/10.1038/nrdp.2017.13

Pothos, E. N., Davila, V., & Sulzer, D. (1998). Presynaptic recording of quanta from midbrain dopamine neurons and modulation of the quantal size. *Journal of Neuroscience*, *18*, 4106–4118. https://doi.org/10.1523/JNEUROSCI.18-11-04106.1998

Rockenstein, E., Nuber, S., Overk, C. R., Ubhi, K., Mante, M., Patrick, C., … Masliah, E. (2014). Accumulation of oligomer-prone alpha-synuclein exacerbates synaptic and neuronal degeneration in vivo. *Brain*, *137*, 1496–1513.

Santo-Domingo, J., & Demaurex, N. (2012). Perspectives on: SGP symposium on mitochondrial physiology and medicine: The renaissance of mitochondrial pH. *Journal of General Physiology*, *139*, 415–423. https://doi.org/10.1085/jgp.201110767

Shults, C. W. (2006). Lewy bodies. *Proceedings of the National Academy of Sciences*, *103*, 1661–1668. https://doi.org/10.1073/pnas.0509567103

Spillantini, M. G., & Goedert, M. (2018). Neurodegeneration and the ordered assembly of alpha-synuclein. *Cell and Tissue Research*, *373*, 137–148.

Spillantini, M. G., Schmidt, M. L., Lee, V. M., Trojanowski, J. Q., Jakes, R., & Goedert, M. (1997). Alpha-synuclein in Lewy bodies. *Nature*, *388*, 839–840.

Surgucheva, I., Newell, K. L., Burns, J., & Surguchov, A. (2014). New alpha- and gamma-synuclein immunopathological lesions in human brain. *Acta Neuropathologica Communications*, *2*, 132.

Taschenberger, G., Toloe, J., Tereshchenko, J., Akerboom, J., Wales, P., Benz, R., … Kügler, S. (2013). beta-synuclein aggregates and induces neurodegeneration in dopaminergic neurons. *Annals of Neurology*, *74*, 109–118.

Tereshchenko, J., Maddalena, A., Bähr, M., & Kügler, S. (2014). Pharmacologically controlled, discontinuous GDNF gene therapy restores motor function in a rat model of Parkinson's disease. *Neurobiology of Diseases*, *65*, 35–42. https://doi.org/10.1016/j.nbd.2014.01.009

Tolö, J., Taschenberger, G., Leite, K., Stahlberg, M. A., Spehlbrink, G., Kues, J., … Kügler, S. (2018). Pathophysiological consequences of neuronal alpha-synuclein overexpression: Impacts on ion homeostasis, stress signaling, mitochondrial integrity, and electrical activity. *Frontiers in Molecular Neuroscience*, *11*.

Touchette, J. C., Breckenridge, J. M., Wilken, G. H., & Macarthur, H. (2016). Direct intranigral injection of dopaminochrome causes degeneration of dopamine neurons. *Neuroscience Letters*, *612*, 178–184. https://doi.org/10.1016/j.neulet.2015.12.028

Ulusoy, A., Bjorklund, T., Buck, K., & Kirik, D. (2012). Dysregulated dopamine storage increases the vulnerability to alpha-synuclein in nigral neurons. *Neurobiology of Diseases*, *47*, 367–377.

Uversky, V. N., Li, J., Souillac, P., Millett, I. S., Doniach, S., Jakes, R., … Fink, A. L. (2002). Biophysical properties of the synucleins and their propensities to fibrillate: Inhibition of alpha-synuclein assembly by beta- and gamma-synucleins. *Journal of Biological Chemistry*, *277*, 11970–11978. https://doi.org/10.1074/jbc.M109541200

Vazin, T., Ball, K. A., Lu, H., Park, H., Ataeijannati, Y., Head-Gordon, T., … Schaffer, D. V. (2014). Efficient derivation of cortical glutamatergic neurons from human pluripotent stem cells: A model system to study neurotoxicity in Alzheimer's disease. *Neurobiology of Diseases*, *62*, 62–72. https://doi.org/10.1016/j.nbd.2013.09.005

Werner-Allen, J. W., Levine, R. L., & Bax, A. (2017). Superoxide is the critical driver of DOPAL autoxidation, lysyl adduct formation, and crosslinking of alpha-synuclein. *Biochemical and Biophysical Research Communications*, *487*, 281–286.

Wilhelm, B. G., Mandad, S., Truckenbrodt, S., Krohnert, K., Schafer, C., Rammner, B., … Rizzoli, S. O. (2014). Composition of isolated synaptic boutons reveals the amounts of vesicle trafficking proteins. *Science*, *344*, 1023–1028. https://doi.org/10.1126/science.1252884

Xu, J., Kao, S. Y., Lee, F. J., Song, W., Jin, L. W., & Yankner, B. A. (2002). Dopamine-dependent neurotoxicity of alpha-synuclein: A mechanism for selective neurodegeneration in Parkinson disease. *Nature Medicine*, *8*, 600–606.

Yamin, G., Munishkina, L. A., Karymov, M. A., Lyubchenko, Y. L., Uversky, V. N., & Fink, A. L. (2005). Forcing nonamyloidogenic beta-synuclein to fibrillate. *Biochemistry*, *44*, 9096–9107.

Zheng, J. H., Viacava Follis, A., Kriwacki, R. W., & Moldoveanu, T. (2016). Discoveries and controversies in BCL-2 protein-mediated apoptosis. *FEBS Journal*, *283*, 2690–2700. https://doi.org/10.1111/febs.13527

SUPPORTING INFORMATION

Additional supporting information may be found online in the Supporting Information section.